

Role of Iron Ion Electron Mediator on Photocatalytic Overall Water Splitting under Visible Light Irradiation Using Z-Scheme Systems

Hideki Kato,¹ Yasuyoshi Sasaki,¹ Akihide Iwase,¹ and Akihiko Kudo*^{1,2}

¹Department of Applied Chemistry, Faculty of Science, Tokyo University of Science, 1-3 Kagurazaka, Shinjuku-ku, Tokyo 162-8601

²Core Research for Evolutional Science and Technology, Japan Science Technology Agency (CREST/JST)

Received June 6, 2007; E-mail: a-kudo@rs.kagu.tus.ac.jp

A combination system consisting of a H₂ production photocatalyst, Pt/SrTiO₃:Rh, and an O₂ production photocatalyst, BiVO₄ or WO₃, decomposed water into H₂ and O₂ under visible light irradiation in the presence of an Fe³⁺/Fe²⁺ redox couple as an electron mediator. O₂ evolution on the BiVO₄ photocatalyst was inhibited by Fe²⁺ ions, because of the oxidation of Fe²⁺ instead of water. In contrast, H₂ evolution on the Pt/SrTiO₃:Rh photocatalyst was enhanced when Fe³⁺ ions co-existed. It is due to the back-reactions between H₂ and O₂ to form water, and the reduction of Fe³⁺ by H₂, which easily proceeded on the bare Pt cocatalyst surface, being efficiently suppressed by adsorption of [Fe(SO₄)(H₂O)₅]⁺ and/or [Fe(OH)(H₂O)₅]²⁺ on the Pt surface. Overall water splitting was achieved with the suppression of the back-reactions even using a Pt cocatalyst. Thus, it clears that iron ions contributed to the present Z-scheme systems not only as an electron mediator but also as an inhibitor of the back-reactions.

Since the first report of photoelectrochemical splitting of water using a semiconductor electrode,¹ the water splitting reaction using photoelectrodes^{2–10} and photocatalysts^{11–18} has been extensively studied for a photon energy conversion. The research has been especially focused on the visible light response with the hopes of utilizing the solar energy. There are some reports on visible-light-driven photoelectrodes.^{4–10} Among them, the GaInP₂/GaAs and dye-sensitized TiO₂/WO₃ tandem electrodes are able to split water without any external voltage.^{6,8} On the other hand, it has been reported that some metal oxide powders with wide band gaps function as active photocatalysts for water splitting.^{11–16} Moreover, it has been recently reported that Ge₃N₄ is the first non-oxide photocatalyst for overall water splitting.¹⁷ Unfortunately, such photocatalysts cannot use sunlight efficiently, because their band gaps are wider than 3 eV. Domen et al. have recently reported overall water splitting under visible light irradiation using a GaN–ZnO solid solution photocatalyst, and its apparent quantum yield is 2.5% at 420–440 nm.¹⁸ On the other hand, there are many reports on H₂ production from water containing an electron donor, such as alcohols and sulfide ions, and O₂ production from water in the presence of an electron acceptor, such as Fe³⁺ and Ag⁺ ions, using metal oxides,^{14,19,20} (oxy)nitrides,²¹ and sulfides^{14,22–24} photocatalysts with visible light responses. The reaction of H₂ or O₂ production from water containing sacrificial reagents is a half reaction of overall water splitting. Therefore, it can be considered that overall water splitting is achieved by systems in which two photocatalysts are active for H₂ and O₂ evolution. The combined systems involving two photoexcitation processes are similar to the photosynthesis system in the green plants, and called “Z-scheme systems.” There are a few reports on water splitting reaction using the Z-scheme system with powdered photo-

catalysts. Fujihara et al. have reported overall water splitting using a two-compartment system.²⁵ In this system, the H₂ evolution compartment involving a Pt/TiO₂ photocatalyst and Br[−] ions as electron donors is connected to the O₂ evolution compartment involving TiO₂ and Fe³⁺ ions as electron acceptors by a Pt wire and an ion-exchange membrane. Sayama et al. have reported the production of H₂ and O₂ from water using the system combined the photochemical H₂ production process using Fe²⁺ under UV light irradiation ($\lambda < 280$ nm) with the photocatalytic O₂ production system of RuO₂/WO₃ with Fe³⁺ ions.²⁶ One-compartment Z-scheme systems constructed of two kinds of photocatalysts, Pt/SrTiO₃:Cr,Ta or Pt/TaON for H₂ evolution and Pt/WO₃ for O₂ evolution, and an IO₃[−]/I[−] redox couple of the electron mediator have been recently reported.^{27–29} In these systems, the overall water splitting reaction proceeds under visible light irradiation. The highest quantum yield of the IO₃[−]/I[−] system is 1% at 420 nm. Thus, the Z-scheme system can be regarded as a candidate for photocatalysis systems aimed at water splitting using sunlight. However, there are significant barriers against its utilization of the solar energy at the present stage. The efficiency of the Z-scheme is still low. Moreover, the useful light is limited with the wavelength shorter than 460 nm, which corresponds to the band gap of the WO₃ photocatalyst.

The authors have recently reported the overall water splitting using some Z-scheme photocatalysis systems, which consist of two kinds of authors' original photocatalysts and an Fe³⁺/Fe²⁺ redox couple as an electron mediator.²⁹ Their quantum yields are 0.4–0.5% at 420 nm. The schematic diagram of the reaction is shown in Fig. 1. On the photocatalyst for O₂ evolution (denoted as O₂-photocatalyst), photogenerated electrons and holes react with Fe³⁺ ions and water to produce Fe²⁺ and O₂, respectively (reactions 1 and 2). On the other hand, on

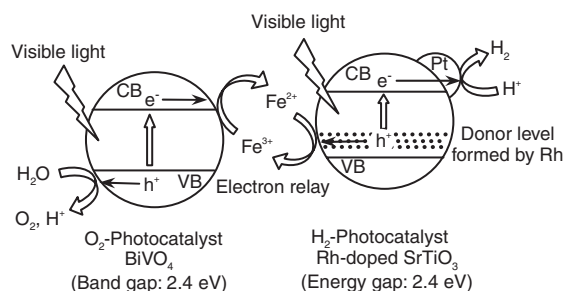
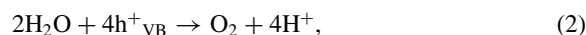


Fig. 1. Overview of overall water splitting on Z-scheme photocatalysis system with an iron ion redox couple.

the photocatalyst for H₂ evolution (denoted as H₂-photocatalyst), photogenerated electrons reduce protons to H₂, and photogenerated holes regenerate Fe³⁺ ions (reactions 3 and 4).



Thus, the Fe³⁺/Fe²⁺ redox couple relays electrons from the O₂-photocatalyst to the H₂-photocatalyst in the present Z-scheme system. The Pt cocatalyst is generally regarded as not effective cocatalyst for water splitting in the powdered photocatalysis system, because it is active for the rapid back-reaction to form water. Moreover, Fe³⁺ ions may inhibit the H₂ production due to capturing of photogenerated electrons in a conduction band of SrTiO₃:Rh and/or to a reaction between H₂ and Fe³⁺ on Pt. However, the present Z-scheme systems were active in overall water splitting in spite of the suspension system using a Pt cocatalyst, implying suppression of the back-reactions on the Pt cocatalyst. Certainly, in other photocatalysis systems involving Pt cocatalysts, overall water splitting has been achieved with efficient suppression of the back reaction by coating with NaOH,¹¹ carbonate,³⁰ and iodine.³¹ Therefore, clarification of the mechanism of suppression of back-reactions on Pt is important for the present systems.

In the present research, effects of pH and the Fe³⁺/Fe²⁺ ratio in a reactant solution on photocatalytic performance of the Z-scheme system and the back-reactions were investigated to clear the role of iron ions. A mechanism of overall water splitting using the Z-scheme system with an iron ion electron mediator is proposed.

Experimental

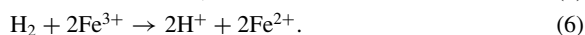
Powders of rhodium-doped SrTiO₃ (denoted as SrTiO₃:Rh) and BiVO₄ were prepared by solid-state and liquid–solid-state reactions, respectively, according to previous literature.^{20a,c} A WO₃ powder was purchased from a chemical company (Nacalai tesque, purity: 99.5%). Deposition of a Pt cocatalyst on SrTiO₃:Rh was carried out using a photodeposition method from H₂PtCl₆. A powder of SrTiO₃:Rh was dispersed in an aqueous methanol solution (10 vol %) containing the appropriate amount of H₂PtCl₆, and then the suspension was irradiated. After photodeposition of the Pt cocatalyst, the Pt/SrTiO₃:Rh powder was filtered, and then washed with water.

Photocatalytic reactions were conducted in a top-window cell

connected to a gas-closed circulation system with on-line gas chromatograph. Photocatalyst powders (50–100 mg for each component) were dispersed into a pH-adjusted aqueous solution containing iron ions. Sulfuric acid or perchloric acid was used to adjust pH of the reactant solution. The reactant solution was stirred with a magnetic stirrer. The temperature of reactant solution was kept at 293 K. Some iron salts, FeCl₂·4H₂O (Wako, purity: 99.9%), FeCl₃·6H₂O (Kanto, purity: 99.0%), Fe(NO₃)₃·9H₂O (Kanto, purity: 99.0%), and Fe₂(SO₄)₃·xH₂O (Wako, purity: 60–80% as Fe₂(SO₄)₃), were used as sources of iron ions. An argon gas (40 Torr) was introduced into the system after deaeration. A 300 W Xe-arc lamp (Parkin-Elmer: Cermex-PE300BF) attached with a sharp cut-off filter (Hoya: L42) was employed for visible light irradiation (λ > 420 nm). Gaseous products were analyzed by using on-line gas chromatograph.

The concentration of an Fe²⁺ ion, C(Fe²⁺), was determined by using colorimetric analysis based on a 1,10-phenanthroline–iron(II) complex.³² For the determination of concentration of Fe³⁺ ions, C(Fe³⁺), Fe³⁺ ions were firstly reduced to Fe²⁺ with hydroxylammonium chloride to determine the whole concentration of iron ions, C(Fe). Then, C(Fe³⁺) was estimated from difference between C(Fe) and C(Fe²⁺).

Back-reactions between H₂ and O₂ to form water and reduction of Fe³⁺ to Fe²⁺ by H₂ (reactions 5 and 6) were investigated. H₂ (20 Torr) and O₂ (10 Torr) were introduced into the reaction system, in which photocatalyst powders and a reactant solution were set as usual photocatalytic reactions except for illumination. Pressure changes were measured in the dark.



Results

Overall Water Splitting on Z-Scheme Photocatalysis Systems with an Fe³⁺/Fe²⁺ Electron Mediator. Overall water splitting reactions under visible light irradiation using a (Pt/SrTiO₃:Rh)–(BiVO₄) system with FeCl₃ or FeCl₂ are shown in Fig. 2. When an aqueous FeCl₃ solution was used, O₂ was dominantly produced at the initial stage of the first run as shown in Fig. 2a. However, the rate of O₂ production decreased gradually. Eventually, H₂ and O₂ were produced in a 2:1 stoichiometric ratio. In a second run after evacuation of gaseous products, H₂ and O₂ were produced in a stoichiometric ratio even at the initial stage. Moreover, the activity, which decreased in the first run, recovered in the initial period of the second run. On the other hand, no gases evolved in the dark. When an aqueous FeCl₂ solution was used, O₂ evolved after 3 h of the reaction time, although the ratio H₂/O₂ (2.7) deviated from stoichiometry. However, H₂ and O₂ were produced in a stoichiometric ratio in the second run. In addition, the rate of H₂ evolution in the second run (20.7 μmol h⁻¹) was higher than that in the first run (12.1 μmol h⁻¹). Thus, overall water splitting proceeded in the both cases of FeCl₃ and FeCl₂. When the reaction proceeded steadily, the concentrations of Fe³⁺ and Fe²⁺ ions were 1.5 and 0.5 mmol L⁻¹, respectively, in the both cases.

Figure 3 shows overall water splitting using a (Pt/SrTiO₃:Rh)–(BiVO₄) system with various iron(III) salts, FeCl₃, Fe(NO₃)₃, and Fe₂(SO₄)₃. Overall water splitting steadily proceeded after an induction period in all cases. No remarkable

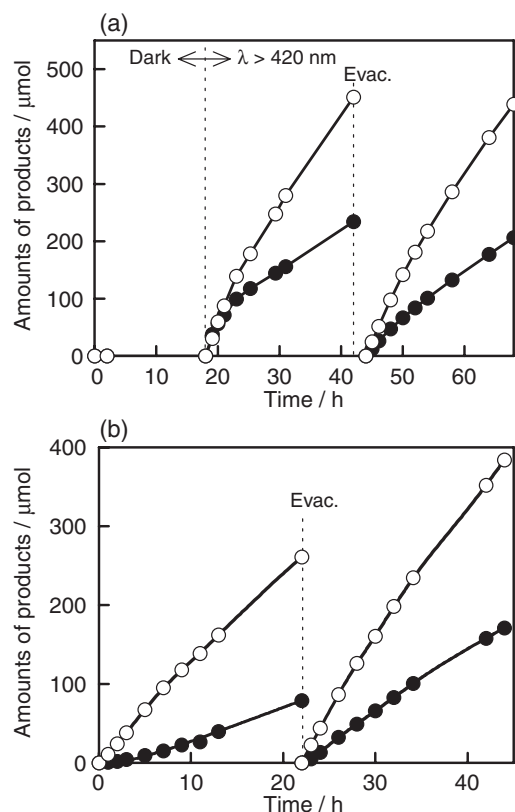


Fig. 2. Photocatalytic overall water splitting using (Pt (0.5 wt %)/SrTiO₃:Rh (1%)-(BiVO₄) system under visible light irradiation in an aqueous solution of (a) FeCl₃ (2 mmol L⁻¹) and (b) FeCl₂ (2 mmol L⁻¹). Open marks: H₂, closed marks: O₂. Catalyst: 0.1 g for each component, reactant solution: 120 mL, pH: 2.4, light source: 300 W Xe-arc lamp with a cut-off filter (λ > 420 nm), cell: top-irradiation cell with a Pyrex window.

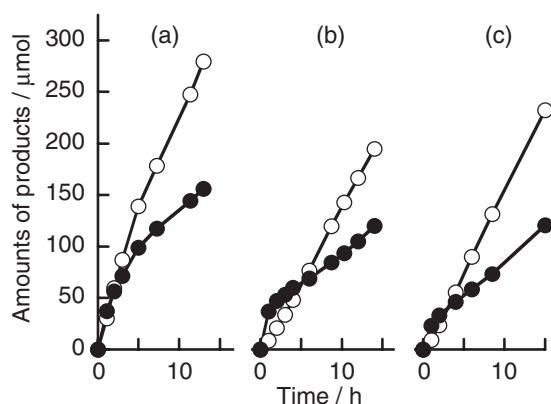


Fig. 3. Photocatalytic overall water splitting over (Pt (0.5 wt %)/SrTiO₃:Rh (1%)-(BiVO₄) system under visible light irradiation in aqueous solutions of (a) FeCl₃, (b) Fe(NO₃)₃, and (c) Fe₂(SO₄)₃. Open marks: H₂, closed marks: O₂. Catalyst: 0.1 g for each component, reactant solution: 2 mmol L⁻¹ of iron, 120 mL, pH: 2.4, light source: 300 W Xe-arc lamp with a cut-off filter (λ > 420 nm), cell: top-irradiation cell with a Pyrex window.

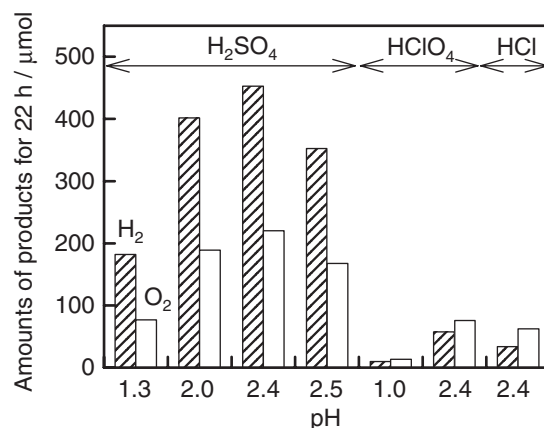


Fig. 4. Dependence of photocatalytic activity of the (Pt (0.5 wt %)/SrTiO₃:Rh (1%)-(WO₃) system on pH under visible light irradiation. Catalyst: 0.1 g for each component, reactant solution: 2 mmol L⁻¹ of FeCl₃, 120 mL, light source: 300 W Xe-arc lamp with a cut-off filter (λ > 420 nm), cell: top-irradiation cell with a Pyrex window.

differences in gas production profiles and photocatalytic activities were observed among three cases.

Figure 4 shows the amounts of gases produced for 22 h of irradiation time over the (Pt/SrTiO₃:Rh)-(WO₃)-(FeCl₃) system with various pH values. Here, the pH was adjusted by sulfuric acid or perchloric acid. The activity of the (Pt/SrTiO₃:Rh)-(WO₃)-(FeCl₃) system was similar to that of the (Pt/SrTiO₃:Rh)-(BiVO₄)-(FeCl₃) system as shown in Figs. 2a and 4. The photocatalytic activity of the present Z-scheme system was sensitive to pH and the kind of acid used for pH control. When sulfuric acid was used for the pH adjustment, the Z-scheme system showed activity in the pH range 1.3–2.5, although the activity depended on the pH. As the pH was increased up to 2.4, the activity increased. However, the activity decreased when the pH was increased to 2.5. On the other hand, when the pH was adjusted with perchloric acid, the Z-scheme system showed activity at pH 2.4, although the activity was only one sixth of that when sulfuric acid was used. When the pH was decreased to 1, the activity was negligible. A similar activity to pH-2.4-FeCl₃-HClO₄ was obtained when the pH was adjusted with hydrochloric acid. The highest activity was obtained in the aqueous FeCl₃-H₂SO₄ solution with pH 2.4.

Absorption spectra of 2 mmol L⁻¹ aqueous FeCl₃ solutions with various pH values, which were adjusted by addition of sulfuric acid or perchloric acid, are shown in Fig. 5. Two absorption bands around 225 and 305 nm were observed for all aqueous FeCl₃-H₂SO₄ solutions. Both absorption bands became small as the pH increased. On the other hand, remarkable change in the absorption profile was observed between pH 1.3 and 2.4 in the aqueous FeCl₃-HClO₄ solution. An absorption maximum was observed at 240 nm in pH-1.3-FeCl₃-HClO₄, whereas an absorption maximum at 210 nm and shoulder peak around 300 nm were observed in pH-2.4-FeCl₃-HClO₄.

Characteristic Properties of the Z-Scheme Systems with an Fe³⁺/Fe²⁺ Electron Mediator. Table 1 lists photocatalytic activity of Pt/SrTiO₃:Rh for H₂ evolution under visible light irradiation from an aqueous FeCl₂ solution with variation

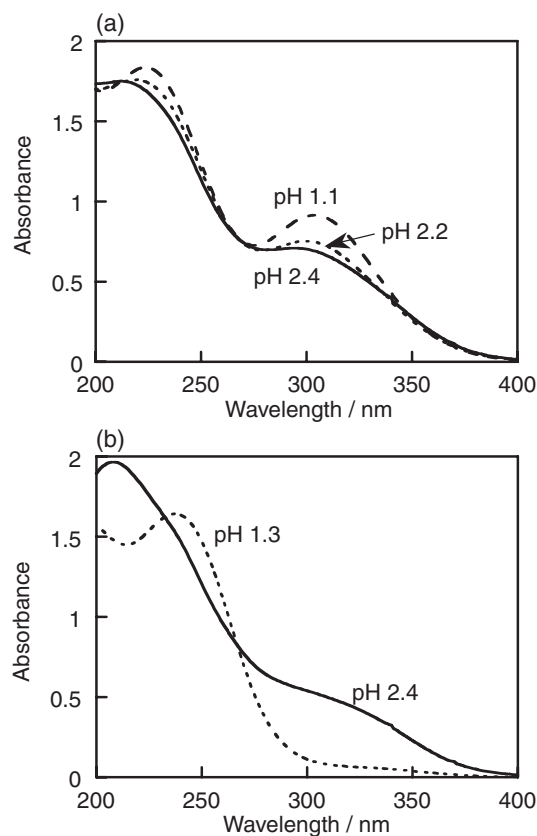


Fig. 5. Absorption spectra of aqueous FeCl_3 solutions (2 mmol L^{-1}) with various pH values; (a) for the solution of $\text{FeCl}_3\text{-H}_2\text{SO}_4$ and (b) for the solution of $\text{FeCl}_3\text{-HClO}_4$. Optical path: 2 mm.

Table 1. Photocatalytic Activity of Pt/SrTiO₃:Rh for H₂ Evolution from an Aqueous Iron Chloride Solution under Visible Light Irradiation^{a)}

Run	Concentration of iron chlorides /mmol L ⁻¹		Rate of H ₂ evolution / $\mu\text{mol h}^{-1}$
	FeCl ₂	FeCl ₃	
1	0	2	ng ^{b)}
2	2	0	8.6
3	2	0.5	9.8
4	2	1	11.1
5	2	2	22.3
6	2	5	23.0
7	0.4	0.4	15.3
8	20	2	11.0

a) Catalyst: 50 mg, reactant solution: 120 mL, pH was adjusted with H_2SO_4 to be 2.4, light source: 300 W Xe lamp with a cut-off filter ($\lambda > 420 \text{ nm}$). b) Negligible.

of the $\text{FeCl}_3/\text{FeCl}_2$ composition. It is a half reaction of the Z-scheme. In an aqueous FeCl_3 solution (Run 1), H₂ evolution was negligible, and no O₂ was produced. In contrast, the Pt/SrTiO₃:Rh photocatalyst produced H₂ in the presence of FeCl_2 (Runs 2–8). H₂ evolution was surprisingly enhanced with an increase in the concentration of coexisting FeCl_3 when the concentration of FeCl_2 was fixed at 2 mmol L^{-1} (Runs 2–6).

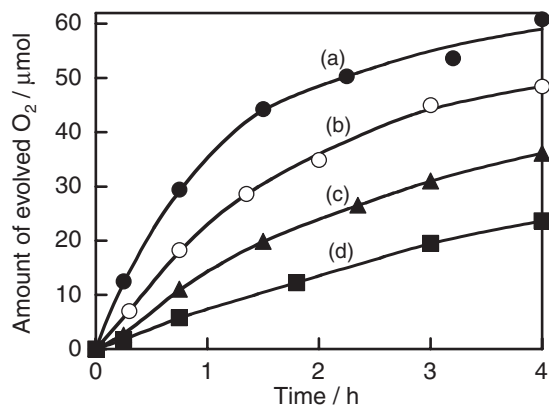


Fig. 6. Photocatalytic O₂ evolution on the BiVO_4 photocatalyst under visible light irradiation in 2 mmol L^{-1} aqueous FeCl_3 solutions with (a) 0, (b) 1, (c) 2, and (d) 5 mmol L^{-1} of FeCl_2 . Catalyst: 0.1 g, reactant solution: 120 mL, pH: 2.4, light source: 300 W Xe-arc lamp with a cut-off filter ($\lambda > 420 \text{ nm}$), cell: top-irradiation cell with a Pyrex window.

In this case, the activity enhancement was significant when the concentration of FeCl_3 was equal to and higher than 2 mmol L^{-1} . However, when the concentration of FeCl_2 was 20 mmol L^{-1} , the activity was not so high even in the presence of FeCl_3 with 2 mmol L^{-1} of the concentration (Run 8). In contrast, relatively high activity was obtained when the ratio of $[\text{Fe}^{3+}]/[\text{Fe}^{2+}]$ was at unity even in the low concentration (Run 7). Thus, the effect of co-presence of FeCl_3 on enhancement of H₂ evolution was significant in the ratio $[\text{Fe}^{3+}]/[\text{Fe}^{2+}] \geq 1$ rather than the concentration of Fe^{3+} .

In contrast to H₂ evolution, the O₂ production on the BiVO_4 photocatalyst was remarkably inhibited by the co-presence of Fe^{2+} ions as shown in Fig. 6. It clearly indicates that oxidation of water to form O₂ competes with oxidation of Fe^{2+} on the BiVO_4 photocatalyst. However, it is noteworthy that BiVO_4 produced O₂ even in the presence of a high concentration, such as 5 mmol L^{-1} , of Fe^{2+} ions. On the other hand, the same activity was obtained when hydrochloric acid was used for pH adjustment instead of sulfuric acid. Thus, the Cl^- ion does not function as a hole scavenger for the BiVO_4 photocatalysts.

Table 2 lists rates of back-reaction (reactions 5 and 6) in the (Pt (0.5 wt %)/SrTiO₃:Rh)-(WO₃) system, which was monitored by observing the decrease in the pressure of H₂ and O₂ in the dark. When iron ions were absent from the solution (Run 1), H₂ and O₂ were consumed in the ratio 2:1 due to the formation of water. In contrast, in the cases of 2 mmol L^{-1} of FeCl_3 , and 1.5 mmol L^{-1} of FeCl_3 with 0.5 mmol L^{-1} of FeCl_2 solutions, of which pH was adjusted to be 2.4 by sulfuric acid (Runs 2 and 4), H₂ was slightly consumed, and the consumption of O₂ was negligible. On the other hand, when the composition of iron ions in the solutions was $[\text{Fe}^{2+}] > [\text{Fe}^{3+}]$ (Runs 7 and 8), H₂ and O₂ were consumed in a 2:1 ratio with the comparable rates to that without iron ions. When the concentration of FeCl_3 was as low as 0.5 mmol L^{-1} (Run 3), the rates of consumption of H₂ and O₂ became higher than those in the case of 2 mmol L^{-1} , but were still lower than those in the absence of iron ions. Interestingly, in this case, the consumption ratio of H₂:O₂ was 3:1. The significant effect of

Table 2. Backward Reaction Rates in the (Pt (0.5 wt %)/SrTiO₃:Rh (1%)-(WO₃) System in the Dark^{a)}

Run	Concentration of iron chloride /mmol L ⁻¹		Acid	pH	Rate of decrease in pressure ^{b)} /Torr h ⁻¹	
	FeCl ₂	FeCl ₃			H ₂	O ₂
1	0	0	H ₂ SO ₄	2.4	2.8	1.4
2	0	2	H ₂ SO ₄	2.4	trace	ng ^{c)}
3	0	0.5	H ₂ SO ₄	2.4	1.1	0.40
4	0.5	1.5	H ₂ SO ₄	2.4	trace	ng ^{c)}
5	0.5	1.5	H ₂ SO ₄	2.0	0.36	0.01
6	0.5	1.5	H ₂ SO ₄	1.3	0.66	0.12
7	1.5	0.5	H ₂ SO ₄	2.4	3.3	1.6
8	2	0	H ₂ SO ₄	2.4	4.1	2.0
9	0	2	HClO ₄	2.4	0.38	0.11
10	0	2	HClO ₄	1.0	2.6	0.09
11	0	2	HCl	2.4	0.47	0.03

a) Catalyst: 0.1 g for each component, solution: 120 mL, gas phase volume: 350 mL. b) Initial pressure: 20 and 10 Torr for H₂ and O₂, respectively. c) Negligible.

addition of FeCl₃ on the suppression of back-reactions was also observed for the (Pt/SrTiO₃:Rh)-(BiVO₄) system.

When the pH value of the solution of 1.5 mmol L⁻¹ FeCl₃ with 0.5 mmol L⁻¹ FeCl₂ became low with addition of sulfuric acid (Runs 4–6), the consumption rates of both H₂ and O₂ became high. Although consumption of O₂ was observed for pH 2.0 and 1.3, the consumption ratio of H₂:O₂ significantly deviated from 2:1, indicating that reduction of Fe³⁺ proceeded in addition to the formation of water.

When perchloric or hydrochloric acid was used to adjust the pH to 2.4 instead of sulfuric acid (Runs 9 and 11), the consumption of H₂ and O₂ was also remarkably suppressed in comparison to the case of the absence of iron ions. However, the consumption of O₂ was still observed, although it was negligible in the case of sulfuric acid. When the pH was decreased to 1 with perchloric acid (Run 10), H₂ was consumed. The rate of consumption was similar to that in the absence of iron ions, whereas O₂ consumption was remarkably suppressed.

The reduction of Fe³⁺ with H₂ (reaction 6) on the Pt/SrTiO₃:Rh was examined in the dark by monitoring the decrease in pressure of H₂ as shown in Fig. 7. The concentration of Fe²⁺ was fixed at 2 mmol L⁻¹, and that of Fe³⁺ was 1 or 5 mmol L⁻¹. The reduction of Fe³⁺ was observed in both cases. The reaction rate based on the consumption of H₂ in the solution with 5 mmol L⁻¹ of Fe³⁺ (0.37 Torr h⁻¹) was one fifth of that with 1 mmol L⁻¹ of Fe³⁺ (1.9 Torr h⁻¹), in spite of the fact that the former contained five times more substrate than the latter. The reaction stopped at 2 h of reaction time in the latter case. It was due to the consumption of Fe³⁺ (120 μmol) contained in the reactant solution. Thus, stoichiometric consumption of H₂ (60 μmol) was confirmed.

Discussion

Overall Water Splitting Using Z-Scheme Systems with Fe³⁺/Fe²⁺ Electron Mediator under Visible Light Irradiation. The system combined with two kinds of photocatalysts, which were active for either H₂ or O₂ formation in the presence of electron donors or acceptors under visible light

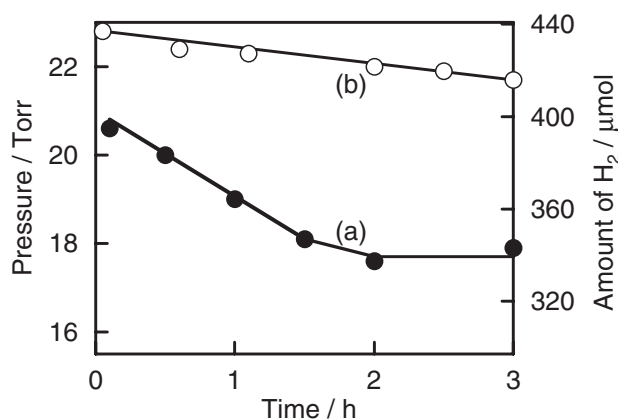


Fig. 7. Decrease in H₂ pressure due to the reaction between H₂ and Fe³⁺ on the Pt (0.3 wt %)/SrTiO₃:Rh photocatalyst in the dark in aqueous solutions; (a) 1 mmol L⁻¹ FeCl₃, 2 mmol L⁻¹ FeCl₂ and (b) 5 mmol L⁻¹ FeCl₃, 2 mmol L⁻¹ FeCl₂. Catalyst: 0.1 g, solution: 120 mL, pH: 2.4, gas phase volume: 350 mL.

irradiation, (Pt/SrTiO₃:Rh)-(BiVO₄), produced H₂ and O₂ in a stoichiometric ratio after an induction period in the presence of iron ions. The activity of the Z-scheme system at steady state was independent of iron salts in the starting solution. The Pt/SrTiO₃:Rh photocatalyst did not produce O₂ from aqueous solutions of FeCl₃ and FeCl₂, whereas H₂ evolution was not observed on the BiVO₄ photocatalyst. Therefore, the production of O₂ or H₂ from the starting solution of FeCl₂ or FeCl₃, respectively, clearly indicated that iron ions functioned as an electron mediator without consumption, according to the Z-scheme as shown in Fig. 1. The concentrations of Fe³⁺ and Fe²⁺ in the steady state were 1.5 and 0.5 mmol L⁻¹, respectively, in both cases of the starting solution of FeCl₃ and FeCl₂. An excess amount of O₂ or H₂ evolved in the induction period was observed when either FeCl₃ or FeCl₂ was used in the starting solution. The (Pt/SrTiO₃:Rh)-(BiVO₄)-(FeCl₃) system produced 890 and 450 μmol of H₂ and O₂, respectively, for 48 h of irradiation time. The number of reacted electron/hole pairs in each photocatalyst was determined to be 1.8 mmol from the amounts of products. It was larger than mole quantities of Pt/SrTiO₃:Rh (545 μmol) and BiVO₄ (275 μmol) photocatalysts used for the reaction. Moreover, it was also larger by 7 times than Fe³⁺ in the reactant solution (240 μmol), proving that iron ions turned over as an electron mediator in the present system. Thus, the results indicate that the overall water splitting proceeds as a Z-scheme photocatalysis process.

Relationship between Photocatalytic Activity and Iron Ion Species in the Solutions. In an aqueous perchloric acid solution, Fe^{III} ions are coordinated by six water molecules, [Fe(H₂O)₆]³⁺, if the pH is low enough. However, [Fe(H₂O)₆]³⁺ is sequentially hydrolyzed to [Fe(OH)(H₂O)₅]²⁺ and [Fe(OH)₂(H₂O)₄]⁺ as the pH increases. Absorption spectra of these Fe^{III} species in an aqueous perchloric acid solution has been reported by Moulik and Gupta.³³ According to the report, [Fe(H₂O)₆]³⁺ and [Fe(OH)(H₂O)₅]²⁺ possess absorption maxima at 240 and 300 nm, respectively. Therefore, the main iron species in the pH-1.3-FeCl₃-HClO₄ solution, which showed an absorption maximum at 240 nm as shown in

Fig. 5b, was assigned to $[\text{Fe}(\text{H}_2\text{O})_6]^{3+}$, and that in the pH-2.4– FeCl_3 – HClO_4 solution, which showed a shoulder peak at 300 nm, was assigned to $[\text{Fe}(\text{OH})(\text{H}_2\text{O})_5]^{2+}$. An intense peak at 210 nm observed in the pH-2.4– FeCl_3 – HClO_4 solution would also be due to $[\text{Fe}(\text{OH})(\text{H}_2\text{O})_5]^{2+}$. The pH-2.4– FeCl_3 – HCl solution gave a quite similar spectrum to pH-2.4– FeCl_3 – HClO_4 , indicating $[\text{Fe}(\text{OH})(\text{H}_2\text{O})_5]^{2+}$ of the main Fe^{III} species (see Supporting Information). On the other hand, $[\text{Fe}(\text{SO}_4)(\text{H}_2\text{O})_5]^+$ and $[\text{Fe}(\text{SO}_4)_2(\text{H}_2\text{O})_4]^-$, which are formed in an aqueous sulfuric acid solution, also possess an absorption maximum at 300 nm as well as $[\text{Fe}(\text{OH})(\text{H}_2\text{O})_5]^{2+}$.³⁴ The absorption peaks observed at 225 and 300 nm in the pH-1.1– and pH-2.2– FeCl_3 – H_2SO_4 solutions should be due to $[\text{Fe}(\text{SO}_4)(\text{H}_2\text{O})_5]^+$ and/or $[\text{Fe}(\text{SO}_4)_2(\text{H}_2\text{O})_4]^-$, because these absorption grew stronger as the concentration of SO_4^{2-} was higher. In the pH-2.4– FeCl_3 – H_2SO_4 solution, absorption in the short wavelength region shifted to 215 nm. It implies that $[\text{Fe}(\text{OH})(\text{H}_2\text{O})_5]^{2+}$, which showed absorption at 210 nm, has a higher concentration in the pH-2.4– FeCl_3 – H_2SO_4 solution than the solutions with pH 1.3 and 2.2. On the other hand, it is thought that $[\text{Fe}(\text{H}_2\text{O})_6]^{3+}$ existed in all solutions according to the equilibrium. The concentration of $[\text{Fe}(\text{H}_2\text{O})_6]^{3+}$ should be larger as the pH decreases.

The pH dependence of activity of the (Pt/SrTiO₃:Rh)–(WO₃)–(FeCl_3) system shown in Fig. 4 can be related to Fe^{III} species in the reactant solution as follows. In the FeCl_3 – H_2SO_4 solutions in which $[\text{Fe}(\text{SO}_4)(\text{H}_2\text{O})_5]^+$, $[\text{Fe}(\text{OH})(\text{H}_2\text{O})_5]^{2+}$, and $[\text{Fe}(\text{H}_2\text{O})_6]^{3+}$ were contained, overall water splitting proceeded in all solutions with 1.3–2.5 of the pH range, although the activity decreased as the pH became low. On the other hand, in the case of FeCl_3 – HClO_4 system, water splitting proceeded in the solution with pH 2.4 which contained both of $[\text{Fe}(\text{OH})(\text{H}_2\text{O})_5]^{2+}$ and $[\text{Fe}(\text{H}_2\text{O})_6]^{3+}$, whereas there was no activity in the solution with pH 1, which contained only $[\text{Fe}(\text{H}_2\text{O})_6]^{3+}$. Therefore, it is thought that $[\text{Fe}(\text{SO}_4)(\text{H}_2\text{O})_5]^+$ or $[\text{Fe}(\text{OH})(\text{H}_2\text{O})_5]^{2+}$ species are indispensable for the present Z-scheme systems to achieve overall water splitting.

Effects of the Ratio of $\text{Fe}^{3+}/\text{Fe}^{2+}$ in the Solution on the Photocatalytic Activities of Half Reactions. O_2 production from water containing Fe^{3+} ions on the BiVO_4 photocatalyst was inhibited by the coexistence of Fe^{2+} ions, as mentioned previously (Fig. 6). Competition of oxidation reactions between water and Fe^{2+} ions is reasonably understood considering the electron donor ability of Fe^{2+} . However, it is noteworthy that the BiVO_4 photocatalyst can produce O_2 even in the presence of Fe^{2+} with 2.5 times higher concentration than Fe^{3+} . Ohno et al. have reported a unique effect of iron ions that adsorption of Fe^{2+} becomes negligible on a TiO_2 photocatalyst when Fe^{3+} coexists.³⁵ It is thought that Fe^{3+} causes the suppression of Fe^{2+} adsorption also for the BiVO_4 photocatalyst, resulting in the suppression of the inhibition from O_2 production by Fe^{2+} . It is preferable property for O_2 -photocatalysts in the Z-scheme systems.

On the other hand, H_2 production from water containing Fe^{2+} ions increased remarkably when Fe^{3+} ions were present in higher concentration than Fe^{2+} ($[\text{Fe}^{3+}] \geq [\text{Fe}^{2+}]$). It is due to that the back-reaction between H_2 and Fe^{3+} (reaction 6) is significantly suppressed when the composition of iron ions in the reactant solution is $[\text{Fe}^{3+}] \geq [\text{Fe}^{2+}]$. The suppression

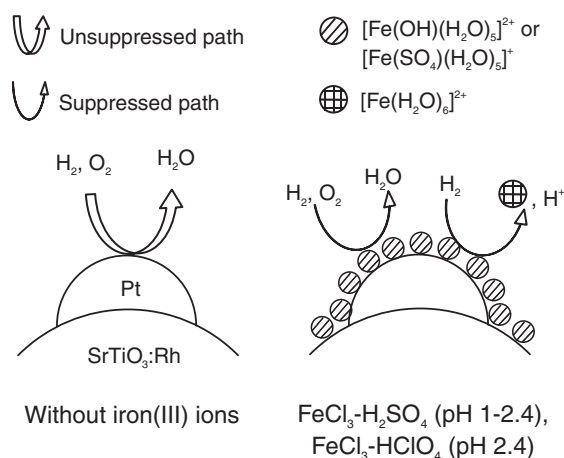


Fig. 8. Suppression of backward reactions by iron(III) ions.

of the back-reaction is probably due to adsorption of Fe^{III} species on the Pt surface. The effect of Fe^{III} species on the back-reactions is further discussed later. The results also indicate that the reduction of Fe^{3+} ions by photogenerated electrons is not dominant on the Pt/SrTiO₃:Rh photocatalyst. In the case of Z-scheme systems with an IO_3^-/I^- electron mediator, H_2 production is eliminated in the presence of small amount of IO_3^- .^{27,28} However, the fact that H_2 production is not inhibited by Fe^{3+} ions is the characteristic feature of the Pt/SrTiO₃:Rh photocatalyst. This feature must contribute to achievement of overall water splitting with the present Z-scheme system using an $\text{Fe}^{3+}/\text{Fe}^{2+}$ electron mediator.

Suppression of Back-Reactions by Iron Ions. The proposed mechanism for the suppression of back-reactions by Fe^{3+} ions from the results (Table 2 and Fig. 7) is illustrated in Fig. 8. From the results listed in Table 2, the rate of water formation can be estimated from the decrease in the O_2 pressure. In addition, the rate of reduction of Fe^{3+} ions by H_2 can also be estimated from the deviation of the consumption ratio from 2:1. Water formation from H_2 and O_2 rapidly proceeds on the surface of Pt when any Fe^{3+} species are absent. In contrast, water formation is significantly suppressed in the presence of Fe^{3+} species if the iron ion composition in the reactant solution is $[\text{Fe}^{3+}] \geq [\text{Fe}^{2+}]$. Such Fe^{3+} species would be adsorbed by not only the SrTiO₃:Rh support but also the Pt surface, resulting in the inhibition of water formation. Thus, Fe^{3+} species adsorbed on the Pt surface suppress water formation as well as NaOH,¹¹ carbonate,³⁰ and iodine.³¹ However, the suppression of water formation is much more efficient in the pH-2.4– FeCl_3 – H_2SO_4 solution than in the pH-2.4– FeCl_3 – HClO_4 and pH-2.4– FeCl_3 – HCl solutions. It is due to the difference in strength of chemisorption between $[\text{Fe}(\text{SO}_4)(\text{H}_2\text{O})_5]^+$ and $[\text{Fe}(\text{OH})(\text{H}_2\text{O})_5]^{2+}$. The $[\text{Fe}(\text{SO}_4)(\text{H}_2\text{O})_5]^+$ ions may bind to Pt via oxygen atoms of the sulfate ligand more strongly than $[\text{Fe}(\text{OH})(\text{H}_2\text{O})_5]^{2+}$ ions. In contrast to the Fe^{3+} species, $[\text{Fe}(\text{H}_2\text{O})_6]^{2+}$ does not suppress water formation. On the other hand, the reduction of Fe^{3+} ions by H_2 of another back-reaction is also remarkably suppressed when the iron ion composition is $[\text{Fe}^{3+}] \geq [\text{Fe}^{2+}]$, except for the pH-1– FeCl_3 – HClO_4 solution, in which $[\text{Fe}(\text{H}_2\text{O})_6]^{3+}$ is the main Fe^{3+} species. Thus, when $[\text{Fe}(\text{SO}_4)(\text{H}_2\text{O})_5]^+$ and/or $[\text{Fe}(\text{OH})(\text{H}_2\text{O})_5]^{2+}$ are the main iron species in the reactant solution,

both back-reactions are remarkably suppressed. However, the efficiency for suppression of reduction of Fe^{3+} by H_2 is different between $[\text{Fe}(\text{SO}_4)(\text{H}_2\text{O})_5]^+$ and $[\text{Fe}(\text{OH})(\text{H}_2\text{O})_5]^{2+}$. It is thought that $[\text{Fe}(\text{SO}_4)(\text{H}_2\text{O})_5]^+$ suppresses the reduction of Fe^{3+} more efficiently than $[\text{Fe}(\text{OH})(\text{H}_2\text{O})_5]^{2+}$ (Runs 2 and 9 in Table 2). On the other hand, the reduction of Fe^{3+} occurred rapidly in the pH-1- FeCl_3 - HClO_4 solution, in which $[\text{Fe}(\text{H}_2\text{O})_6]^{3+}$ is the main Fe^{3+} species. It indicates that $[\text{Fe}(\text{H}_2\text{O})_6]^{3+}$ does not inhibit the adsorption of H_2 on Pt. Then, $[\text{Fe}(\text{H}_2\text{O})_6]^{3+}$ is reduced instead of O_2 . The increase in the rates of back-reactions by decreasing the pH, observed in the FeCl_3 - H_2SO_4 solutions, is due to the increase in the concentration of $[\text{Fe}(\text{H}_2\text{O})_6]^{3+}$ (Runs 4–6 in Table 2). As described above, it has been found that back-reactions on the Pt surface are efficiently suppressed by $[\text{Fe}(\text{OH})(\text{H}_2\text{O})_5]^{2+}$ and/or $[\text{Fe}(\text{SO}_4)(\text{H}_2\text{O})_5]^+$. It is a characteristic feature of the present Z-scheme systems that iron ions contribute to water splitting not only as the electron mediator but also as an inhibitor of the back-reactions.

The back-reactions should be suppressed by a decrease in sites for the dissociative adsorption of H_2 and in the mobility of the dissociated hydrogen on the Pt surface due to the adsorption of Fe^{3+} species, such as $[\text{Fe}(\text{SO}_4)(\text{H}_2\text{O})_5]^+$ and $[\text{Fe}(\text{OH})(\text{H}_2\text{O})_5]^{2+}$. Therefore, it is concluded that the suppression of reduction of Fe^{3+} with H_2 by adsorption of Fe^{3+} is the main reason for the promotion of H_2 production with increasing in the concentration of Fe^{3+} ions as listed in Table 1. The promotion of H_2 production accompanied by the increase in the concentration of Fe^{3+} ions is somewhat strange from the viewpoint of electron acceptability of Fe^{3+} . However, the positive effect of Fe^{3+} on suppression of the back-reaction should overcome the negative effect of Fe^{3+} on the trapping of photogenerated electrons.

The pH dependence of photocatalytic activity of the present Z-scheme system for water splitting (Fig. 4) can be explained in terms of the back-reactions as follows. The back-reactions proceed faster as the pH of the reactant solution becomes lower (Table 2). Therefore, the decrease in the suppression of back-reactions due to an increase in the concentration of $[\text{Fe}(\text{H}_2\text{O})_6]^{3+}$ is the main reason for the pH dependence of activity. On the other hand, the decrease in the activity in the pH 2.5 solution is due to the collapse of active site by adsorption of the $\text{FeO}(\text{OH})$ colloid, which is caused by the pH increase.

As described above, the rates of back-reactions are strongly dependent upon the iron species in the reactant solution in the present Z-scheme system using an $\text{Fe}^{3+}/\text{Fe}^{2+}$ electron mediator. $[\text{Fe}(\text{SO}_4)(\text{H}_2\text{O})_5]^+$ and/or $[\text{Fe}(\text{OH})(\text{H}_2\text{O})_5]^{2+}$ effectively suppress such back-reactions in comparison with $[\text{Fe}(\text{H}_2\text{O})_6]^{3+}$. It is concluded that the suppression of back-reactions significantly contributes to achievement of overall water splitting by construction of the Z-scheme system in spite of using a Pt cocatalyst.

Conclusion

Photocatalytic water splitting into H_2 and O_2 in a stoichiometric ratio under visible light irradiation was possible by using a Z-scheme system composed of two kinds of visible-light driven photocatalysts, Pt/SrTiO₃:Rh and BiVO₄ or WO₃,

and iron ions of an electron mediator. It has been experimentally demonstrated that the iron ions turned over as an electron mediator. The presence of Fe^{2+} inhibited O_2 production on the BiVO₄ photocatalyst. On the other hand, H_2 production on the Pt/SrTiO₃:Rh photocatalyst increased when Fe^{3+} was presented in a higher concentration than Fe^{2+} .

The back-reactions of water formation and reduction of Fe^{3+} on the Pt surface were remarkably suppressed in the presence of Fe^{3+} ions. The suppression of the back-reactions depended on the kind of iron species in the reactant solution. It is clear from analysis of the back-reactions in the dark that the most effective iron species for suppression of back-reactions is $[\text{Fe}(\text{SO}_4)(\text{H}_2\text{O})_5]^+$. In addition, the suppression of back-reactions was significant when the concentration of Fe^{3+} was higher than that of Fe^{2+} .

The composition of iron ions in the reactant solution was $[\text{Fe}^{3+}] > [\text{Fe}^{2+}]$ in the steady state of the overall water splitting reaction. In addition, the highest activity was obtained when $[\text{Fe}(\text{SO}_4)(\text{H}_2\text{O})_5]^+$ was the main Fe^{3+} species. Thus, the conditions needed to suppress the back-reactions efficiently were determined, resulting in overall water splitting, in spite of using the Pt cocatalyst.

This work was supported by the Core Research Evolutional Science and Technology (CREST), and Grant-in-Aids for the Priority Area (No. 417) and for Young Scientists (No. 17750135) from the MEXT of the Japanese Government.

Supporting Information

Absorption spectrum of a pH-2.4- FeCl_3 - HCl solution. This material is available free charge on the Web at: <http://www.csj.jp/journals/bcsj>.

References

- 1 A. Fujishima, K. Honda, *Nature* **1972**, 238, 37.
- 2 H. Yoneyama, H. Sakamoto, H. Tamura, *Electrochem. Acta* **1975**, 20, 341.
- 3 A. B. Ellis, S. W. Kaiser, M. S. Wrighton, *J. Phys. Chem.* **1976**, 80, 1325.
- 4 G. Campet, M. P. Dare-Edwards, A. Hamnett, J. B. Goodenough, *Nouv. J. Chim.* **1980**, 4, 501.
- 5 M. Matsumura, M. Hiramoto, H. Tsubomura, *J. Electrochem. Soc.* **1983**, 130, 326.
- 6 O. Khaselev, J. A. Turner, *Science* **1998**, 280, 425.
- 7 S. U. M. Khan, J. Akikusa, *J. Phys. Chem. B* **1999**, 103, 7184.
- 8 M. Grätzel, *Nature* **2001**, 414, 338.
- 9 C. Santato, M. Ulmann, J. Augustynski, *J. Phys. Chem. B* **2001**, 105, 936.
- 10 S. U. M. Khan, M. Al-Shahry, W. B. Ingler, Jr., *Science* **2002**, 297, 2243.
- 11 S. Sato, J. M. White, *Chem. Phys. Lett.* **1980**, 72, 83.
- 12 J. M. Lehn, J. P. Sauvage, R. Ziessel, *Nouv. J. Chim.* **1980**, 4, 623.
- 13 K. Domen, J. N. Kondo, M. Hara, T. Takata, *Bull. Chem. Soc. Jpn.* **2000**, 73, 1307.
- 14 A. Kudo, H. Kato, I. Tsuji, *Chem. Lett.* **2004**, 33, 1534.
- 15 a) S. Ogura, M. Kohno, K. Sato, Y. Inoue, *Appl. Surf. Sci.* **1997**, 121–122, 521. b) M. Kohno, T. Kaneko, S. Ogura, K. Sato, Y. Inoue, *J. Chem. Soc., Faraday Trans.* **1998**, 94, 89. c) J. Sato,

- N. Saito, H. Nishiyama, Y. Inoue, *J. Phys. Chem. B* **2003**, *107*, 7965.
- 16 H. Kato, K. Asakura, A. Kudo, *J. Am. Chem. Soc.* **2003**, *125*, 3082.
- 17 J. Sato, N. Saito, Y. Yamada, K. Maeda, T. Takata, J. N. Kondo, M. Hara, H. Kobayashi, K. Domen, Y. Inoue, *J. Am. Chem. Soc.* **2005**, *127*, 4150.
- 18 a) K. Maeda, T. Takata, M. Hara, N. Saito, Y. Inoue, H. Kobayashi, K. Domen, *J. Am. Chem. Soc.* **2005**, *127*, 8286. b) K. Maeda, K. Teramura, D. Lu, T. Takata, N. Saito, Y. Inoue, K. Domen, *Nature* **2006**, *440*, 295.
- 19 J. R. Darwent, A. Mills, *J. Chem. Soc., Faraday Trans. 2* **1982**, *78*, 359.
- 20 a) A. Kudo, K. Omori, H. Kato, *J. Am. Chem. Soc.* **1999**, *121*, 11459. b) T. Ishii, H. Kato, A. Kudo, *J. Photochem. Photobiol., A* **2004**, *163*, 181. c) R. Konta, T. Ishii, H. Kato, A. Kudo, *J. Phys. Chem. B* **2004**, *108*, 8992. d) R. Niishiro, H. Kato, A. Kudo, *Phys. Chem. Chem. Phys.* **2005**, *7*, 2241.
- 21 a) G. Hitoki, A. Ishikawa, T. Takata, J. N. Kondo, M. Hara, K. Domen, *Chem. Lett.* **2002**, 736. b) G. Hitoki, T. Takata, J. N. Kondo, M. Hara, H. Kobayashi, K. Domen, *Chem. Commun.* **2002**, 1698. c) A. Kasahara, K. Nukumizu, G. Hitoki, T. Takata, J. N. Kondo, M. Hara, H. Kobayashi, K. Domen, *J. Phys. Chem. A* **2002**, *106*, 6750.
- 22 T. Sakata, in *Heterogeneous Photocatalysis at Liquid–Solid Interfaces in Photocatalysis*, ed. by N. Serpone, E. Pelizzetti, Wiley, New York, **1984**, p. 311.
- 23 a) I. Tsuji, H. Kato, H. Kobayashi, A. Kudo, *J. Am. Chem. Soc.* **2004**, *126*, 13406. b) I. Tsuji, H. Kato, A. Kudo, *Angew. Chem., Int. Ed.* **2005**, *44*, 3565. c) I. Tsuji, H. Kato, H. Kobayashi, A. Kudo, *J. Phys. Chem. B* **2005**, *109*, 7323.
- 24 A. Ishikawa, T. Takata, J. N. Kondo, M. Hara, H. Kobayashi, K. Domen, *J. Am. Chem. Soc.* **2002**, *124*, 13547.
- 25 K. Fujihara, T. Ohno, M. Matsumura, *J. Chem. Soc., Faraday Trans.* **1998**, *94*, 3705.
- 26 K. Sayama, R. Yoshida, H. Kusama, K. Okabe, Y. Abe, H. Arakawa, *Chem. Phys. Lett.* **1997**, *277*, 387.
- 27 a) K. Sayama, K. Mukasa, R. Abe, Y. Abe, H. Arakawa, *Chem. Commun.* **2001**, 2416. b) K. Sayama, K. Mukasa, R. Abe, Y. Abe, H. Arakawa, *J. Photochem. Photobiol., A* **2002**, *148*, 71. c) R. Abe, K. Sayama, H. Sugihara, *J. Phys. Chem. B* **2005**, *109*, 16052.
- 28 R. Abe, T. Takata, H. Sugihara, K. Domen, *Chem. Commun.* **2005**, 3829.
- 29 H. Kato, M. Hori, R. Konta, Y. Shimodaira, A. Kudo, *Chem. Lett.* **2004**, *33*, 1348.
- 30 K. Sayama, H. Arakawa, *J. Chem. Soc., Faraday Trans.* **1997**, *93*, 1647.
- 31 R. Abe, K. Sayama, H. Arakawa, *Chem. Phys. Lett.* **2003**, *371*, 360.
- 32 W. B. Fortune, M. G. Mellon, *Ind. Eng. Chem., Anal. Ed.* **1938**, *10*, 60.
- 33 S. P. Moulik, K. K. S. Gupta, *J. Indian Chem. Soc.* **1972**, *49*, 447.
- 34 R. A. Whiteker, N. Davidson, *J. Am. Chem. Soc.* **1953**, *75*, 3081.
- 35 T. Ohno, D. Haga, K. Fujihira, M. Matsumura, *J. Phys. Chem. B* **1997**, *101*, 6415.